Off-centering of hydrogenic impurities in quantum dots

J. L. Movilla and J. Planelles*
Departament de Ciències Experimentals, UJI, Box 224, E-12080 Castelló, Spain
(Received 3 August 2004; revised manuscript received 13 December 2004; published 22 February 2005)

We report exact numerically calculated ground state and binding energies of a hydrogenic donor impurity confined everywhere inside a spherical quantum dot (QD) surrounded by air or a vacuum. Finite spatial steplike potentials allowing the electronic density to partially leak outside the QD are considered. This model faces a divergence produced by the self-polarization potential at the position of the dielectric mismatch. We bypass it by replacing the edge steplike dielectric mismatch by a continuous variation within an extremely thin layer at this edge. A comprehensive study of several confining factors influencing electronic and binding energies is carried out and a highly nonadditive interplay is found. Our calculations show that within both the strong and weak confinement regimes we may be faced with three different *behavior regimes*. We call them *low, intermediate*, and *high*. In the low and intermediate behaviors, the mass, polarization, and self-polarization effects exert a very strong influence on the electron density distribution, so that perturbational estimations of the binding energy may not be appropriate even in the strong confinement regime. These low and intermediate behavior regimes are responsible for binding energy profiles not being monotonously decreasing vs off-centering. It is even theoretically possible to design systems with off-centering independent binding energies.

DOI: 10.1103/PhysRevB.71.075319 PACS number(s): 71.55.−i, 73.21.La, 73.22.−f

I. INTRODUCTION

A deep understanding of the effects of impurities on electronic states of semiconductor nanostructures is a fundamental question in semiconductor physics because their presence can dramatically alter the performance of quantum devices.[1]

The binding energy (E_b) of shallow donor impurities in nanoscopic systems depends upon materials and geometry (size and shape), although it seems that shape has a minor influence.[2,3] The position of the impurity also has a strong influence.[4–6] By assuming homogeneous distribution of impurities in spherical quantum dots (QDs), Silva *et al.*[7] have shown that impurities located next to the QD edge govern the absorption spectra, a second smaller peak emerging for large QDs which is associated with transitions involving impurities at the QD center.

Spatial confinement increases E_b with respect to the impurity in the bulk as it pushes up the allowed energies and also because it reduces the size-dependent static dielectric constant.[8,9] However, this last indirect effect is very small for QDs larger than 1 or 2 nm.[10,11] In addition, we can increase E_b by including the spatially dependent screening of an impurity ion caused by the valence electrons,[12] but again this E_b increment only amounts to a few meV, except for extremely small QDs.[13,14]

A major contribution to E_b comes from polarization charges caused by the dielectric mismatch at the QD edge. If the internal ϵ_i static dielectric constant is larger than the external ϵ_o one, then the induced charge has the same sign as the impurity, yielding an attractive interaction with the electron and, therefore, an appreciable increase in E_b. If $\epsilon_o > \epsilon_i$, the opposite holds.[10,15–17] The dielectric mismatch at the QD edge also produces an additional dielectric effect, the so-called self-energy, i.e., the interaction between the electron and its induced polarization. Almost all calculations accounting for these polarization effects assume that the carriers are confined inside the QD by an infinite barrier. This may be a reasonable model for crystallites in vacuum, air, or a solvent (but definitely not for a QD embedded in a semiconductor matrix with a materials band offset that is not very large). The infinite confinement potential has the practical advantage of yielding a wave function that is zero at the QD edge, thus eluding the divergence produced by self-potential at the edge (originating from the steplike dielectric mismatch). This divergence is not integrable, since it is pathological for the Schrödinger equation. Regularized self-energy, i.e., a linear interpolation replacing the actual self-energy in a thin layer at the interface of the order of a lattice constant, has been employed with finite spatial confining potentials[18] (the underlying assumption is that the electrodynamics of continuous media breaks down in the microscopic domain and that the above-mentioned interpolation is a good average). It should be mentioned that this regularized self-energy does not have a proper scaling with size. An alternative model for self-energy having a correct scaling and simultaneously eluding divergences has been suggested.[11,19] In this model the dielectric mismatch is replaced by a continuous variation of the dielectric constant within a thin layer located at the interface. This self-energy model has an analytical solution for spherical QDs that can be written as an infinite, rather slowly convergent, series.

Exact solutions for hydrogenic donors located at the center of spherical QDs have been obtained,[20–24] while variational[5–7,10,13,14,20,25–30] and perturbational calculations[9,16,17,31,32] have been carried out for on- and off-centered impurities. In the present paper, we employ the self-energy model of continuous change of dielectric constant at the QD edge, assume a realistic, finite confining potential, and carry out exact (numerical) calculation on ground state and binding energies of spherical QDs with off-centered impurities, including polarization and self-energy terms. The aim of the paper is the study of the interplay of different factors influencing binding energy. These factors include the

direct Coulomb term, the spatial confinement coming from the band offsets, the confinement produced by hydrostatic strain, the differences in effective masses in different media, polarization induced by discontinuities in the static dielectric constant, and electron self-energy coming from differences in dynamic or optical dielectric constants in different media. We exclude donor self-energy because this interaction contributes to the donor formation energy when the donor is introduced into the QD. We consider both weak ($R > a_0^*$) and strong ($R < a_0^*$) confinement regimes, a_0^* and R being the effective Bohr and QD radii, respectively. We prove that it is important to carry out exact calculations for a proper comparison of the results obtained. We will show that by tuning the different sources of interactions (tailoring) we can design a QD including a donor impurity whose off-centering may stabilize, unstabilize, or almost have no effect on the binding energy. Since there is nowadays widespread interest in the research of new materials with very high or very low dielectric constants,[33–39] our results may stimulate specific research into these new materials in order to design new nanoscopic devices.

II. THEORETICAL OUTLINE

We consider spherical semiconductor nanocrystals and study the effect of off-centering a shallow donor impurity on the electronic ground state and binding energies. The hydrogenic energy levels can be well described by the effective mass approach (EMA) down to nanocrystallite sizes of the order of 2 nm (Refs. 10 and 40). The corresponding Hamiltonian (a.u.) reads

$$\mathcal{H} = -\frac{1}{2}\nabla\left(\frac{1}{m^*(\mathbf{r})}\nabla\right) + V(\mathbf{r}) + \phi_c + \phi_s. \tag{1}$$

The first term is the Hermitian kinetic energy operator for a position-dependent mass.[41] $V(\mathbf{r})$ is given by

$$V(\mathbf{r}) = \begin{cases} 0 & \text{if } r < R, \\ V_0 & \text{if } r \geqslant R. \end{cases} \tag{2}$$

Here V_0 is the dot-matrix band offset. Since we deal with spherical nanocrystals, the strain comes into the Hamiltonian Eq. (1) just by modifying the value V_0 and, indirectly, by a slight modification of the electron effective mass.[42,43]

ϕ_c is the Coulomb term, including polarization effects. We employ a macroscopic treatment, the validity of which has been well established for semiconductor QDs.[11] The analytical expression of ϕ_c for an exciton in a multishell spherical nanocrystal is explicitly given in Ref. 11 as an infinite series in terms of the Legendre polynomials. We have particularized this expression for an electron interacting with an off-centered donor ion (a centered hydrogenic impurity is a straightforward and well-known particular case). Without loss of generality, we assume that the donor ion is located on the z axis (at a distance z_0 from de QD center), and write ϕ_c in cylindrical coordinates. Since z_0 is a fixed position, ϕ_c only depends on the ρ and z coordinates of the electron. In the case of a quantum dot in a matrix, ϕ_c can be written in the following form:

$$\phi_c^{1,1}(z_0;\rho,z) = \phi_A + \phi_B + \phi_C, \quad r < R, \tag{3}$$

$$\phi_c^{1,2}(z_0;\rho,z) = \phi_D + \phi_E, \quad r > R, \tag{4}$$

with

$$\phi_A = -\frac{1}{\epsilon_i}\sum_{l=0}^{\infty} P_l(\cos\gamma)\left(\frac{r_<}{r_>}\right)^l \frac{1}{r_>}, \tag{5}$$

$$\phi_B = -\frac{\epsilon_i - \epsilon_0}{\epsilon_i \epsilon_0}\frac{1}{R}, \tag{6}$$

$$\phi_C = -\frac{1}{\epsilon_i}\sum_{l=1}^{\infty} P_l(\cos\gamma)\left(\frac{(l+1)(\epsilon_i - \epsilon_0)}{\epsilon_0(l+1) + \epsilon_i l}\frac{1}{R}\left(\frac{r_>}{R}\frac{r_<}{R}\right)^l\right), \tag{7}$$

$$\phi_D = -\frac{1}{\epsilon_0}\frac{1}{r_>}, \tag{8}$$

$$\phi_E = -\frac{1}{\epsilon_0}\sum_{l=1}^{\infty} P_l(\cos\gamma)\frac{1}{r_>}\left(\frac{r_<}{r_>}\right)^l\left(1 + \frac{l(\epsilon_0 - \epsilon_i)}{\epsilon_0(l+1) + \epsilon_i l}\right), \tag{9}$$

where $r_<(r_>)$ is the smallest (greatest) absolute value between $r = \sqrt{\rho^2 + z^2}$ and z_0. Indoors, ϕ_A is the direct Coulomb term, ϕ_B is the polarization potential of an on-center impurity, and ϕ_C is the polarization correcting term coming from off-centering. Outdoors, ϕ_D is the potential corresponding to an on-center impurity and ϕ_E is the corresponding off-centering correction.

In order to achieve accuracy, the above-mentioned Legendre polynomials have been calculated at each coordinated value by a recurrence formula.[44]

ϕ_s is the electron self-polarization energy, which can be obtained from ϕ_c (Ref. 11). The implementation of this self-potential for a quantum dot in a matrix (two regions and then two different dielectric constants) or a multishell quantum dot (several regions with different dielectric constants) yields divergences at the interfaces. As is stated in the Introduction, divergences arise at the positions where the $\epsilon(\mathbf{r})$ profile has a steplike discontinuity. We then assume a continuous cosinelike model for $\epsilon(\mathbf{r})$ across a thin 3 Å layer at the interface.[11,19] However, since we carry out numerical integration, the cosinelike model will be discretized to yield a multistep profile. Then, we use a discretization scheme that avoids calculating at the dielectric discontinuities.[45] This scheme eludes every divergence and mimics the continuous variation of the dielectric constant. A convenient rewriting of the ϕ_s expression in Ref. 11 is also carried out in order to elude the low convergence and numerical inaccuracy coming from computational cutoff errors.[45]

Summing up, we obtain a differential equation only dependent on two electron coordinates (ρ and z) and including the following kinetic energy operator:

$$\hat{T} = -\frac{1}{2\rho}\frac{\partial}{\partial\rho}\left(\frac{\rho}{m^*(\rho,z)}\frac{\partial}{\partial\rho}\right) - \frac{1}{2}\frac{\partial}{\partial z}\left(\frac{1}{m^*(\rho,z)}\frac{\partial}{\partial z}\right), \tag{10}$$

where $m^*(\rho,z)$ is the steplike variable effective mass. In order to elude the source of inaccuracy arising from the

δ-function nature of $\partial m^*/\partial\rho$ and $\partial m^*/\partial z$, we discretize Eq. (10) (using central finite differences) following the scheme proposed by Harrison,[46] which ensures the robustness of the method even for large changes in the effective mass across the interfaces.

The discretization of Eq. (1) yields eigenvalue problems of asymmetric, huge, and sparse matrices. Energies and wave functions are obtained by means of diagonalizations. To this end we use the Arnoldi solver[47] implemented in the ARPACK package.[48]

III. NUMERICAL RESULTS

In this section we study the influence of different confinement sources on the energy and E_b of an electron trapped by an impurity located in a QD surrounded by air or vacuum ($\epsilon_o = m_o^* = 1$). This is the environment where the dielectric effects are expected to be the largest. Exploratory calculations on the isolated contribution of each confining source on the ground state of the system show that an external effective mass (m_o^*) higher than that of the QD (m_i^*) leads to an energy stabilization vs the impurity off-centering $z_I = z_o/R$. This can be easily understood in terms of the kinetic contribution to the energy: A higher effective mass in the external region, where the wave function is still different from zero, translates into a minor kinetic energy and, then, a lower total energy. As the impurity gets closer to the edge a larger amount of electronic density spreads over the QD surrounding medium and, thus, a higher energy stabilization occurs.

A similar reasoning led us to the conclusion that the spatial confining potential provided by the band offset induces an energy unstabilization as z_I increases.

The contribution of the ϕ_c term in Hamiltonian Eq. (1) to the ground state energy of the system is stabilizing, its action increasing with z_I when $\epsilon_i > \epsilon_o$. However, the off-centering stabilization capability of ϕ_c is ϵ_i dependent. It has been found[45] that the largest contribution to the energy differences between on-center and off-center impurities occurs when employing dielectric constants of about $\epsilon_i = 3$ (assuming $\epsilon_o = 1$).

Self-polarization ϕ_s enhances these energy differences: In the case of $\epsilon_i > \epsilon_o$, this potential looks like a small, almost constant, barrier inside the QD, and a deep and narrow well outside, by the QD edge.[11] As we move the impurity from the center towards the crystallite border, an increasing amount of electron density comes into the deep, stabilizing well of the self-polarization potential.

However, the previous off-center stabilizing effects can be drastically reduced by the spatial confining potential, as it may prevent the wave function from leaking outside the QD. In the next subsection we will show that these confinement effects are highly nonadditive so that specific interplays will yield singular behaviors, such as an increasing or decreasing of E_b as the impurity is being off-centered.

A. Off-centering of a hydrogenic impurity in a SiO_2 nanocrystal: A paradigmatic case of weak confinement regime

As pointed out in the Introduction, we may find in the literature many variational calculations on the ground state and binding energies (E_b) of donor impurities located everywhere in QDs that have been modeled by parabolic and steplike confining potentials (with both finite and infinite barriers).[5–7,20,25–27] To our knowledge all these calculations deal with systems where the dielectric mismatch is small, so that polarization and self-polarization effects have been neglected. A second common feature of these calculations is that they include situations in which the studied system is in the weak confinement regime, where perturbational methods are not suitable and, thus, the variational approach is a good alternative. In the present paper, we carry out exact (numerical) calculations and will show that in some situations this is about the only reliable tool.

A general trend found in all the above-mentioned studies is that the ground state E_b always diminishes as z_I increases. A simple reasoning emerges: the closer the impurity is to the QD edge, the higher the amount of electronic density close to the unstabilizing potential barrier will be. Nevertheless, our preliminary studies lead us to suspect that at least some specific interplays may yield an opposite trend for E_b (an off-centering stabilization due to $m_i < m_0$ and $\epsilon_i > \epsilon_0$). It has been determined that, for a crystallite in air or vacuum, the highest energy variation vs z_I occurs for values of the dielectric constant $\epsilon_i \approx 3$. Then, the study of a SiO_2 nanocrystal (with static dielectric constant $\epsilon_s = 4$) may be of special interest. We consider next a spherical $R = 3$ nm SiO_2 nanocrystal in air. The material parameters employed are effective mass $m_i^* = 0.5$ (Ref. 49), electroaffinity $EA = 0.9$ eV (Ref. 50), static dielectric constant $\epsilon_s = 4$ (Ref. 17), and dynamic or optical dielectric constant $\epsilon_\infty = 2$ (Ref. 51). The effective Bohr radius is, then, $a_0^* = a_0 \epsilon_s / m^* = 4.2$ Å $\ll R$, i.e., the confinement regime of the nanocrystal is clearly weak.

We carry out two series of calculations of E_b vs z_I, which are shown in Fig. 1(a), namely, S0 (dotted line) excluding self-energy and S1 (full line) including self-energy calculated using the (appropriate[53]) optical ϵ_∞ dielectric constant.[54] The spatial confinement step potential height is assumed to equal electroaffinity.[52] Binding energy E_b, as commonly defined, is the difference between the ground state energy of a QD without and with impurity.

As we suspected, Fig. 1(a) shows that E_b increases with z_I. It is just the opposite to the generally accepted trend of E_b vs z_I. This is a new, relevant result of this work. In other words, despite the unstabilizing spatial confining potential, the interplay with mass, polarization, and self-polarization yields stabilization as z_I increases.

One may think that the relatively small SiO_2 electroaffinity ($EA = 0.9$ eV) and, therefore, the relatively shallow spatial confining potential (0.9 eV high) may be the reason for the calculated anomalous E_b vs z_I behavior. Indeed, most semiconductors have $EA \approx 4$ eV. Thus, we repeat the above calculation but artificially increase the spatial confining barrier up to 10 eV (higher than those of most semiconductors). The results are shown in Fig. 1(b). We can see there that from $z_I = 0$ up to $z_I \approx 0.7$ E_b increases (the electron density does not feel the barrier yet). Nevertheless, larger values of z_I involve a decrease in E_b. We will discuss the interplay of factors influencing E_b in greater detail later in the paper.

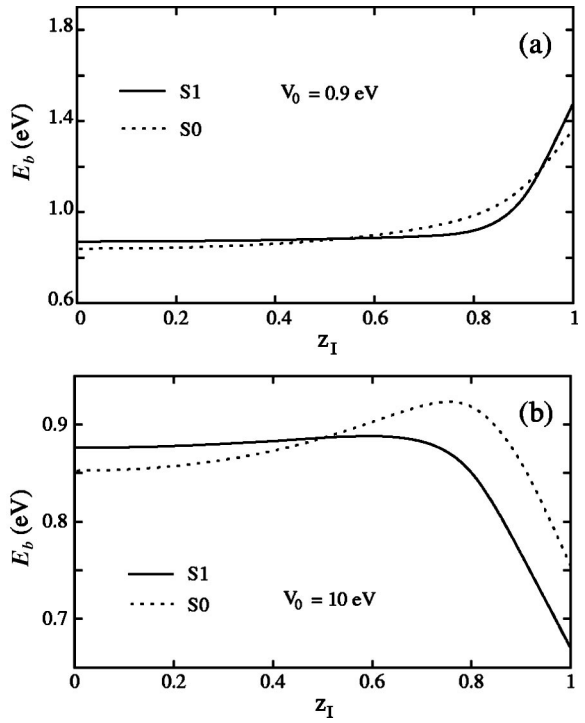

FIG. 1. (a) Ground state binding energy vs impurity off-centering z_I corresponding to a $R=3$ nm spherical SiO_2 nanocrystal in air or vacuum ($m_o^*=\epsilon_o=1$). Calculations have been performed without (S0, dotted line) and with the inclusion of the self-polarization contributions (S1, full line). SiO_2 parameters are specified in the text. (b) Same as (a) but with $V_0=10$ eV and the self-polarization potential that is now calculated with $\epsilon_i=4$ and $\epsilon_0=1$.

B. Strong confinement regime: exact calculations vs perturbational approach

Small crystallites built of materials with large dielectric constants and light effective masses are in the strong confinement regime ($R<a_0^*$). For calculating binding energies in these nanocrystals, including full dielectric effects, Ferreyra *et al.*[17,32] have developed the so-called strong confinement approach[55] and have carried out calculations employing two models of spatial confining potential, namely parabolic and infinite hard wall, and for both on- and off-centered impurities. Their results show that the strong confinement approach yields meaningful results in all the cases studied, from which a general trend seems to emerge: E_b is a monotonous decreasing function of z_I (the same result as the one found in the variational calculations discussed in the previous subsection).

In order to check whether the strong confinement approach can be generalized to the (more realistic) finite steplike spatial confining potential, we carry out the same calculation as in the previous subsection (SiO_2 in vacuum) but, this time, we have artificially reduced the effective mass to $m^*=0.05$, in order to move into the strong confinement regime. The results are shown in Fig. 2(a), where we can see that if E_b is calculated numerically excluding self-energy (S0) it is almost insensitive to the off-centering, while this is not the case when self-energy is included (S1). This is so because for $z_I>0.7$ the attractive self-polarization potential

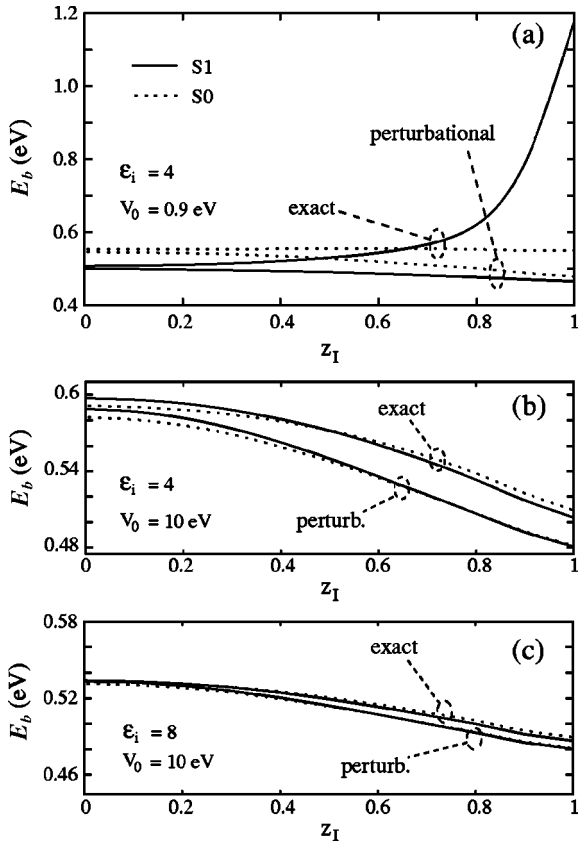

FIG. 2. (a) Exact and first-order perturbational estimations of binding energy E_b vs off-centering z_I for a $R=3$ nm spherical QD in air or vacuum ($m_i^*=0.05$, $m_0^*=1$, $\epsilon_i=4$, $\epsilon_o=1$ and $V_0=0.9$ eV). S1 (full lines) include while S0 (dotted lines) exclude self-polarization contributions. The zeroth-order wave functions employed in the perturbational calculations are those of the impurity-free QD in the presence and absence of the self-polarization potential, respectively. (b) Same as (a) but with $V_0=10$ eV and $\epsilon_i=4$. (c) Same as (a) but with $V_0=10$ eV and $\epsilon_i=8$.

well squeezes part of the electronic density into the well, yielding a relevant increase in E_b. The differences we find out between S0 and S1 and the fact that exact E_b increases with z_I lead us to suspect that the first-order perturbation approach would not be appropriate in this case. On the one hand, the self-polarization potential ϕ_s has not first-order contribution to E_b and, on the other hand, the Coulomb ϕ_c term always predicts a reduction in E_b vs z_I (Refs. 17 and 31). This steady prediction can be explained as follows: in the strong confinement approach E_b is calculated as the opposite sign expectation value of the ϕ_c potential, Eqs. (3)–(9), in the impurity free QD ground state. The angular part of the corresponding wave function is just a constant $Y_0^0(\theta,\phi)=1/\sqrt{4\pi}$. Thus, when integrating over the angular coordinates, only the terms $P_l(\cos\gamma)$ of ϕ_c contain the angular (θ,ϕ) variables. Since

$$P_l(\cos\gamma)=\frac{4\pi}{2l+1}\sum_{m=-l}^{m=l}Y_l^m(\theta_0,\phi_0)^*Y_l^m(\theta,\phi), \qquad (11)$$

where (θ_0,ϕ_0) are the (fixed) coordinates of the impurity and

$$\frac{1}{\sqrt{4\pi}}\langle Y_l^m(\theta,\phi)\rangle = \langle lm|00\rangle = \delta_{l,0}\delta_{m,0}, \tag{12}$$

we have $\langle P_l(\cos\gamma)\rangle = 4\pi\delta_{l,0}\delta_{m,0}$. Therefore, only the $l=0$ terms in Eqs. (3)–(9) contribute to the expectation value. It works as if ϕ_c would be reduced to

$$\phi_c^{1,1}(l=0) = -\frac{1}{\epsilon_i r_>} - \frac{\epsilon_i-\epsilon_0}{\epsilon_i\epsilon_0}\frac{1}{R},\ r<R, \tag{13}$$

$$\phi_c^{1,2}(l=0) = -\frac{1}{\epsilon_0 r_>},\ r>R, \tag{14}$$

where $r_>=r$ if $r>z_0$ and $r_>=z_0$ if $r<z_0$, $(\rho=0,z_0)$ being the impurity location. In other words, only $\phi_c^{1,1}$ depends on z_0, and this dependence (the larger z_0 is, the shallower $\phi_c^{1,1}$ will be) always leads to a decrease in E_b vs z_I.

The previous reasoning also helps to understand why the perturbational approach works quite well for on-center ($z_I=0$) impurities and deteriorates as z_I increases [see Fig. 2(a)]. Indeed, if $z_I=0$, Eqs. (3)–(9) reduce to Eqs. (13) and (14), with $r_>$ replaced by r, so that by calculating the expectation value we do not actually neglect any term coming from higher order perturbation theory, which is not the case if $z_I\neq 0$.

We may describe the results in Fig. 2(a) as a balance between polarization potential (stabilization) and spatial confining potential (unstabilization) yielding an E_b that is almost insensitive to off-centering [see S0 series in Fig. 2(a)]. When self-energy (stabilization) comes into play, then a net increase in E_b vs z_I results. We may reverse the situation by increasing the spatial confining potential. This is the case plotted in Fig. 2(b), where a huge 10 eV potential barrier (felt almost like infinity by the ground state) is present. In this case the strong confinement approach works well even at z_I close to one. It should be mentioned that in this case self-energy has almost no influence on E_b.

By looking at the numerical wave function it can be seen that the huge spatial confining potential prevents the electronic density from leaking into the self-polarization potential well. Thus, a double stabilizing effect is switched off; on the one hand, the stabilization coming from the self-potential itself and, on the other hand, the effect of the external mass (reducing the kinetic energy). We can say that both self-energy and mass effects almost vanish, so that the small differences between exact and perturbationally calculated E_b come from the off-center polarization correcting term ϕ_C, Eq. (7), which first-order perturbational contribution to E_b is zero but, obviously, makes a nonzero contribution to the exact E_b if $z_I\neq 0$.

Above we stated that the sensitivity of E_b to a change in z_I is maximum around $\epsilon_i=3$. It is connected to the fact that $|\phi_C|$ [Eq. (7)] also has a maximum around this value of ϵ_i (Ref. 45). In the above calculation $\epsilon_i=4$. A larger ϵ_i is expected to mean a smaller $|\phi_C|$, i.e., a better performance of the perturbational approach. This is shown in Fig. 2(c).

C. Binding energy vs band offset

In the above subsections we have shown three different E_b vs z_I profiles. In this subsection we will show that the above-mentioned profiles correspond to the three possible *behavior regimes* we may meet as we increase the spatial confining potential. We will refer them to as *low, medium*, and *high* behavior regimes, although the border between consecutive regimes, i.e., the corresponding potential height, will be very much dependent on the other factors (dielectric constants ϵ_i and ϵ_0, effective masses m_i^* and m_0^*).

For the sake of clarity, we will fix the effective masses ($m_i^*=0.2$ and $m_0^*=1$) in order to diminish the number of variables in our study. Then we carry out three series of calculations including high $\epsilon_i=16$ (like ϵ_{Ge}), medium $\epsilon_i=8$ (like ϵ_{ZnO}), and low $\epsilon_i=4$ (like $\epsilon_{\mathrm{SiO_2}}$) internal dielectric constants and an external $\epsilon_o=1$ (corresponding to vacuum or air). We scan spatial confining potential heights V_0 from near zero up to $V_0=4$ eV (which covers most semiconductors). We plot E_b vs V_0 for different off-centerings ($z_I=0$, 0.4, 0.6, 0.8, and 0.9). Finally, in order to see the effect of self-energy, we again carry out two series of calculations: S0 (dotted lines) without self-energy[56] and S1 (full lines) full calculation. The nanocrystal radius, as in the above subsections, is fixed to $R=3$ nm.

Figure 3(a) displays the results corresponding to the low $\epsilon_i=4$ dielectric constant and the above-mentioned behavior regimes can be seen. In the range $0<V_0<1.6$ eV E_b is a monotonously increasing function of z_I. In the range $V_0>2.5$ eV E_b is a monotonously decreasing function of z_I. Finally, in the intermediate region $1.6<V_0<2.5$ eV, E_b first increases vs z_I, then reaches a maximum and finally decreases.

All the same, Fig. 3(a) reveals that self-polarization is crucial to determine the behavior regime regions. Thus, S0 calculations predict a $0<V_0<2.2$ eV low region, and a medium one extending from 2.2 up to $V_0>4$ eV, the highest potential included in our calculations.

Finally, it is worthwhile pointing out that the effective mass $m_i^*=0.2$ and the dielectric constant $\epsilon_i=4$ employed in all calculations included in Fig. 3(a) yield an effective Bohr radius $a_0^*=10.5$ Å, which means that we are in the weak confinement regime. All the same, all three possible E_b behavior regimes are encountered here.

The next two sets of calculations, namely those for $\epsilon_i=8$ and $\epsilon_i=16$, represent a transit towards the strong confinement regime ($a_0^*=2.1$ nm and $a_0^*=4.2$ nm vs $R=3$ nm, respectively). The results are shown in Figs. 3(b) and 3(c). Again all three E_b vs z_I behavior regimes arise; the most remarkable feature is that by increasing ϵ_i a shrinking of the intermediate region occurs, so that for high values of ϵ_i it almost disappears and becomes just a dot between low and high behavior regions. Turning this the other way round, we see that for high dielectric constants we may find a potential V_0 for which E_b does not depend on z_I. This is another relevant result of this work that may beuseful in technological applications: since impurities may appear almost randomly in

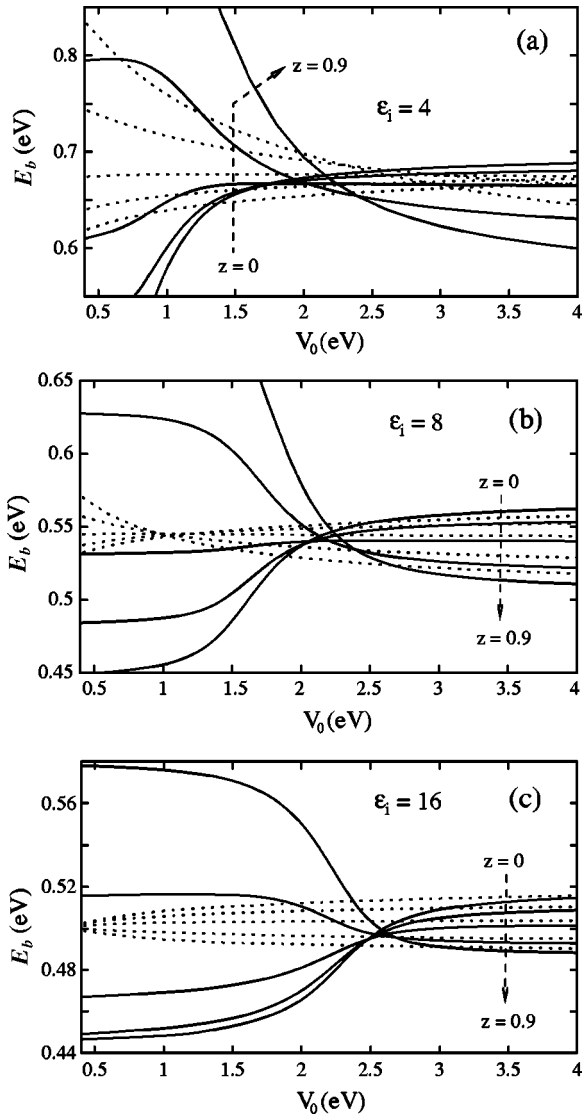

FIG. 3. (a) Ground state binding energy vs spatial confinement V_0 corresponding to a $R=3$ nm, $\epsilon_i=4$, $m_i^*=0.2$ spherical QD in air or vacuum ($m_o^*=\epsilon_o=1$). Results for $z_I=0.0$, 0.4, 0.6, 0.8, and 0.9 are displayed following the order indicated by the auxiliary arrow. Full (dotted) lines correspond to calculations including (excluding) self-polarization effects. (b) Same as (a) but with $\epsilon_i=8$. (c) Same as (a) but with $\epsilon_i=16$.

different locations within the QD and since electronic properties depend on their location, they are usually a nuisance. However, doping with impurities in a z_I-independent material may be useful in the design of nanoelectronic devices.

Finally, we would underline another relevant result that can be seen in Figs. 3(a)–3(c): self-energy has a huge influence on E_b in the low behavior region, while its influence is small for high potentials. From a practical point of view this means that we should not use perturbational estimations of self-energy in the low and intermediate behavior regimes, with the additional difficulty that the borders of these regions cannot be established in general (they depend on ϵ_i, ϵ_0, m_i^*, m_0^* and also the QD radius). The reliability of E_b first-order perturbational estimations published to date is connected with the negligible role played by self-energy on E_b when infinite spatial potential models are employed[9,16,17,31,32].

IV. CONCLUDING REMARKS

Using exact (numerical) integration, we have reported calculated ground state and binding energies of a donor confined everywhere inside a spherical QD surrounded by air or vacuum. A comprehensive study of several confining factors influencing electronic and binding energies is carried out. We find a highly nonadditive interplay that to a large extent makes it difficult to assess general behavior trends.

Our calculations show that within both, the strong and the weak confinement regime, three different *behavior regimes* may occur, and that in the low and intermediate behaviors, the mass, polarization, and self-polarization effects influence the electron density distribution so much that we cannot safely carry out perturbational estimations of the binding energy. Then, we conclude that a strong regime of confinement cannot always guarantee a safe estimation of binding energies by means of first-order perturbation theory (strong confinement approach).

These low and intermediate behavior regimes have not been reported so far in the literature and, as we show in this paper, they are responsible for the $E_b(z_I)$ profiles that are different from the always monotonously decreasing previously reported (in both cases, strong and weak confinement regimes). We also show that it is possible to tune an off-centering independent E_b, which can be of technological interest in designing new nanoelectronic devices.

ACKNOWLEDGMENTS

Financial support from MEC-DGI Project No. CTQ2004-02315/BQU and UJI-Bancaixa Project No. P1-B2002-01 are gratefully acknowledged. A MECD of Spain FPU grant is also acknowledged (JLM).

*Electronic address: planelle@exp.uji.es

[1] *Mesoscopic Physics and Electronics*, edited by T. Ando, Y. Arakawa, K. Foruka, S. Komiyama, and H. Nakashima (Springer, Berlin, 1998); H. J. Queisser and E. E. Haller, Science **281**, 945 (1998).
[2] F. J. Ribeiro and A. Latgé, Phys. Rev. B **50**, 4913 (1994).
[3] P. G. Bolcatto and C. R. Proetto, Phys. Rev. B **59**, 12 487 (1999).
[4] G. Bastard, Phys. Rev. B **24**, 4714 (1981).
[5] J. L. Zhu and X. Chen, Phys. Rev. B **50**, 4497 (1994).
[6] N. Porras-Montenegro, S. T. Pérez-Merchancano, and A. Latgé, J. Appl. Phys. **74**, 7624 (1993).
[7] J. Silva-Valencia and N. Porras-Montenegro, J. Appl. Phys. **81**, 901 (1997).
[8] D. R. Penn, Phys. Rev. **128**, 2093 (1962).

[9] M. Lannoo, C. Delerue, and G. Allan, Phys. Rev. Lett. **74**, 3415 (1995).
[10] R. Tsu and D. Babić, Appl. Phys. Lett. **64**, 1806 (1994).
[11] P. G. Bolcatto and C. R. Proetto, J. Phys.: Condens. Matter **13**, 319 (2001).
[12] J. Hermanson, Phys. Rev. **150**, 660 (1966).
[13] H. Paredes-Gutiérrez, J. C. Cuero-Yépez, and N. Porras-Montenegro, J. Appl. Phys. **75**, 5150 (1994).
[14] Z. Y. Deng, J. K. Guo, and T. R. Lai, Phys. Rev. B **50**, 5736 (1994).
[15] L. E. Brus, J. Chem. Phys. **80**, 4403 (1984).
[16] M. Iwamatsu and K. Horii, Jpn. J. Appl. Phys., Part 1 **36**, 6416 (1997).
[17] J. M. Ferreyra and C. R. Proetto, Phys. Rev. B **52**, R2309 (1995).
[18] L. Bányai and S. W. Koch, *Semiconductor Quantum Dots* (World Scientific, Singapore, 1993).
[19] F. Stern, Phys. Rev. B **17**, 5009 (1978).
[20] J. L. Zhu and X. Chen, J. Phys.: Condens. Matter **6**, L123 (1994).
[21] J. L. Zhu, J. J. Xiong, and B. L. Gu, Phys. Rev. B **41**, 6001 (1990).
[22] J. L. Zhu, Phys. Rev. B **39**, 8780 (1989).
[23] V. Ranjan and V. A. Singh, J. Appl. Phys. **89**, 6415 (2001).
[24] F. Qu, M. Alcalde, C. G. Almeida, and N. O. Dantas, J. Appl. Phys. **94**, 3462 (2003).
[25] A. Corella-Madueño, R. Rosas, J. L. Marín, and R. Riera, J. Appl. Phys. **90**, 2333 (2001).
[26] Z. Xiao, J. Zhu, and F. He, J. Appl. Phys. **79**, 9181 (1996).
[27] C. Bose, J. Appl. Phys. **83**, 3089 (1998).
[28] Z. Y. Deng, J. K. Guo, and T. R. Lai, J. Phys.: Condens. Matter **6**, 5949 (1994).
[29] N. Porras-Montenegro and S. T. Pérez-Merchancano, Phys. Rev. B **46**, 9780 (1992).
[30] H. Ham and H. N. Spector, J. Appl. Phys. **93**, 3900 (2003).
[31] G. Allan, C. Delerue, M. Lannoo, and E. Martin, Phys. Rev. B **52**, 11 982 (1995).
[32] J. M. Ferreyra, P. Bosshard, and C. R. Proetto, Phys. Rev. B **55**, 13 682 (1997).
[33] K. Maex, M. R. Baklanov, D. Shamiryan, F. Iacopi, S. H. Brongersma, and Z. S. Yanovitskaya, J. Appl. Phys. **93**, 8793 (2003).
[34] H. Treichel and C. Goonetilleke, Adv. Eng. Mater. **3**, 461 (2001).
[35] S. Yu, T. K. S. Wong, K. Pita, and X. Hu, J. Vac. Sci. Technol. B **20**, 2036 (2002).
[36] E. J. Osten, E. Bugiel, and A. Fissel, Solid-State Electron. **47**, 2161 (2003).
[37] S. A. Campbell, H. S. Kim, D. C. Gilmer, B. He, T. Ma, and W. L. Gladfelter, IBM J. Res. Dev. **43**, 383 (1999).
[38] C. J. Forst, C. R. Ashman, K. Schwarz, and P. E. Blochl, Nature (London) **427**, 53 (2004).
[39] D. A. Buchanan, IBM J. Res. Dev. **43**, 243 (1999).
[40] W. Jaskólski and G. W. Bryant, Phys. Rev. B **57**, R4237 (1998); C. Priester, G. Allan, and M. Lannoo, *ibid.* **28**, 7194 (1983).
[41] D. BenDaniel and C. B. Duke, Phys. Rev. **152**, 683 (1966).
[42] D. Bimberg, M. Grundmann, and N. N. Ledentsov, *Quantum Dot Heterostructures* (Wiley, Chichester, 2001).
[43] M. Califano and P. Harrison, Phys. Rev. B **61**, 10 959 (2000).
[44] G. Arfken, *Mathematical Methods for Physicists* (Academic, San Diego, 1985).
[45] J. L. Movilla and J. Planelles (unpublished).
[46] P. Harrison, *Quantum Wells, Wires and Dots* (Wiley, Chichester, 2001).
[47] W. E. Arnoldi, Q. Appl. Math. **9**, 17 (1951); Y. Saad, *Numerical Methods for Large Scale Eigenvalue Problems* (Halsted Press, New York, 1992); R. B. Morgan, Math. Comput. **65**, 1213 (1996).
[48] R. B. Lehoucq, K. Maschhoff, D. C. Sorensen, P. A. Vu, and C. Yang, *ARPACK: FORTRAN subroutines for solving large scale eigenvalue problems, Release 2.1*, available at http://www.caam.rice.edu/software/ARPACK; R. B. Lehoucq, D. C. Sorensen, and C. Yang, *ARPACK User's Guide: Solution of Large-Scale Eigenvalue Problems with Implicit Restarted Arnoldi Methods* (SIAM, Philadelphia, 1998).
[49] Z. A. Weinberg, J. Appl. Phys. **53**, 5052 (1982).
[50] J. Robertson, J. Vac. Sci. Technol. B **18**, 1785 (2000).
[51] F. Gustini, P. Umari, and A. Pasquarello, Microelectron. Eng. **72**, 299 (2004).
[52] R. L. Anderson, Solid-State Electron. **5**, 341 (1962); J. L. Shay, S. Wagner, and J. C. Phillips, Appl. Phys. Lett. **28**, 31 (1976).
[53] The response of a dielectric medium to an impurity fixed in a QD site (static) is properly accounted for by the static dielectric constant. However, when calculating the self-polarization potential of a fast moving electron we should take into account that the electron moves too rapidly for the atom cores to adjust, so phonons cannot be involved. Hence, dynamic ϵ_∞ should be employed.
[54] By completely off-centered, $z_I=1$, impurity we actually mean an impurity located at $(R-h/2)$, where R is the QD radius and h is the discretization of the grid (see Section II).
[55] Basically this approach is a first order perturbation calculation of E_b using the ground state of an impurity-free QD as the zeroth-order wave function.
[56] Since the calculations do not correspond to any specific material, we have no criterion to determine the value of optical dielectric constant ϵ_∞ and for the sake of simplicity we always employ ϵ_s unless otherwise indicated.